

## **Influence of X-ray Radiation on the Phase Composition and Morphology of Electric Furnace Slag, Clinker, and Plaster**

*Alenka Rastovčan-Mioč,<sup>a,\*</sup> Štefica Cerjan-Stefanović,<sup>b</sup>  
Vjera Novosel-Radović,<sup>c</sup> Boro Mioč,<sup>d</sup> and Tahir Sofilić<sup>c</sup>*

*<sup>a</sup> Faculty of Metallurgy, University of Zagreb,  
Aleja narodnih heroja 3, 44103 Sisak, Croatia*

*<sup>b</sup> Faculty of Chemical Engineering and Technology, University of Zagreb,  
Marulićev trg 19, 10000 Zagreb, Croatia*

*<sup>c</sup> Sisak Steelworks, Božidara Adžije 19, 44010 Sisak, Croatia*

*<sup>d</sup> Felis d.o.o., Božidara Adžije 19, 44010 Sisak, Croatia*

Received June 7, 2000; revised January 5, 2001; accepted February 8, 2001

The effect of X-ray irradiation upon the structure and morphology of samples of clinker, plaster, and electric furnace slag was studied. Slag was obtained in the process of austenite manganese steel casting. The research objective was to determine the stability of these materials under radiation.

The changes that occurred were analyzed by X-ray diffraction and scanning electron microscopy. The diffractograms show changes in the profile, number, relative intensity of diffraction lines, and measured width values at half the maximum height. The micrographs show swelling and cracking of grains. As the radiation time was prolonged, this phenomenon became more evident, which points to the apparent change in the size and shape of the slag, clinker, and plaster grains, *i.e.* the elementary components of cement.

*Key words:* cement, electric furnace slag, clinker, plaster, radiation.

---

\* Author to whom correspondence should be addressed.

## INTRODUCTION

Slags from iron and steel industries are sometimes classified as industrial waste material. Today these by-products are valuable and extremely versatile construction materials. Potential fields of slag application have been extended over the past few years, mostly for environmental and economic reasons. Construction industry has applied predominantly granulated slag, obtained by quick cooling of molten blast-furnace slag, basic-oxygen furnace steel slag and magnesium slag. Quick cooling is performed with large volumes of running water or a slag jet is subjected to a water jet, *i.e.* air-water jet. Such slag hardens like glass and it can be used as a raw material for the production of clinker or as an additive to Portland cement. Slag can also be used as a potential replacement for Portland cement in concrete. In the production of clinker, slag can be used as raw material in the cooled lumpy form although it hardens to a crystalline stone material and is better used in the road construction.<sup>1,2</sup>

Today, due to the ever increasing share of electric steel worldwide, *i.e.* reduced production of iron in blast-furnaces, steel mill slag is gaining more and more significance and is replacing blast-furnace slag in numerous fields of application.<sup>3,4</sup> In metallurgy, steel mill slag is used as iron provider and flux and it can also be used as construction material. It is very successfully applied in forestry, agriculture, glass industry, wool industry and in the production of water purification filter media.

The starting point of this work was the presumption that slag is used as an additive in the construction industry. Such an application of slag must deal with the potential problem: aging of construction material is a consequence of its exposure to weather or to radiation. The effects of these influences may not be visible at first, but in the course of time they lead to structural changes, which directly affect the mechanical properties of the material.<sup>5-7</sup>

Therefore, this research included the influence of X-ray radiation upon samples of electric furnace slag,\* Portland cement clinker,\*\* and technical plaster\*\*\* (cement ingredients). The phase composition and morphology of the samples were examined before and after exposure to X-ray radiation for 1, 3, and 5 hours. X-ray diffraction analysis and scanning electron microscopy were applied.

---

\* Hereinafter referred to as : slag.

\*\* Hereinafter referred to as : clinker.

\*\*\* Hereinafter referred to as : plaster.

## EXPERIMENTAL

### *Samples*

Samples of slag, clinker, and plaster were examined.

The slag sample was obtained in the production of austenite manganese steel in the basic electric arc furnace (at 1883 K) at the »Felis« Foundry in Sisak. The sample was taken with a spoon onto a plate and slowly cooled with a small quantity of water. (Although this procedure resulted in a crystalline structure, it is equivalent to the structure of most slag materials at waste deposits). The cold sample (294 K) was ground and homogenized for 150 minutes in a Herzog vibration mill. Successive quartering and crushing of the cold sample provided 100 g of sample.

Samples of clinker (Portland cement clinker made of high carbonate and low carbonate raw materials) and plaster (technical stone) were supplied by the »Našice-cement« Cement Factory.

All samples were dried for 2 hours at 378 K and stored in a desiccator above silica gel.

Part of the samples were placed as thin films on Mylar foil in the sample holder Philips PW 1427/40. They were irradiated for 1, 3 or 5 hours in the X-ray spectrometer, Philips PW 1410/10 (Au – anode, 25 mA, 50 kV). The resulting structural and morphological changes were examined by X-ray diffraction and scanning electron microscopy.

### *Procedures*

*Chemical Analysis:* Chemical composition of the samples was examined with standard chemical procedures.<sup>8,9</sup>

*X-ray Diffraction Analysis:* In order to determine the phase composition of unirradiated and irradiated slag, clinker, and plaster samples, the method of X-ray diffraction was applied. All samples were prepared in a standard procedure.<sup>10</sup>

X-ray diffraction powder patterns were taken at room temperature using a counter diffractometer with monochromatized Cr-K $\alpha$  radiation (Philips diffractometer, proportional counter and graphite monochromator). Diffraction intensities of the 004 reflection (Mn,Mg)<sub>2</sub>SiO<sub>4</sub> (slag), 312 reflection 3CaO · SiO<sub>2</sub> (clinker) and 123 reflection CaSO<sub>4</sub> · 2H<sub>2</sub>O (plaster) were measured and the full-width at half-maximum (FWHM) was determined.

In the present work, phases were identified according to the data in the ICDD Powder Diffraction File (cards: 4–0326, 12–432, 14–376, 1–1127, 14–77, 11–273, 12–145, 12–284, 10–139, 13–209, 13–534, 6–0046, 2–1124, 6–0046, 5–0586, 8–133, 11–179, 5–0490 i 15–776).<sup>11</sup> Other phases were identified according to Narita.<sup>12</sup>

*Scanning Electron Microscopy:* The morphology of irradiated samples of slag, clinker, and plaster was determined by means of a scanning electron microscope. The scanning electron microscopy samples were attached to a support with colloidal silver and coated with an evaporated layer of copper in a JEOL type evaporator. Electron micrographs were taken on a JEOL JXA 50A scanning electron microscope.

## RESULTS AND DISCUSSION

The chemical composition of slag, clinker, and plaster samples was analyzed. The phase composition and morphology of these samples were examined before and after their exposure to X-rays for one, three, and five hours.

Results of the quantitative chemical analysis are shown in Table I.

TABLE I  
Mass fraction / % of slag, clinker, and plaster

Slag		Clinker		Plaster	
SiO <sub>2</sub>	31.25	SiO <sub>2</sub>	20.76	CaSO <sub>4</sub> ·2H <sub>2</sub> O + CaSO <sub>4</sub> ·1/2H <sub>2</sub> O	91.24
Fe <sub>2</sub> O <sub>3</sub>	2.00	Fe <sub>2</sub> O <sub>3</sub>	2.81	Fe <sub>2</sub> O <sub>3</sub>	0.50
CaO	13.21	CaO	65.32	CaCO <sub>3</sub>	3.83
MgO	16.24	MgO	1.81	MgCO <sub>3</sub>	2.34
K <sub>2</sub> O	0.85	K <sub>2</sub> O	0.72	Al <sub>2</sub> O <sub>3</sub>	0.38
Na <sub>2</sub> O	0.26	Na <sub>2</sub> O	0.23	SiO <sub>2</sub> + insoluble	1.45
Mn <sub>2</sub> O <sub>3</sub>	35.97	Al <sub>2</sub> O <sub>3</sub>	5.89		
P <sub>2</sub> O <sub>5</sub>	0.048	loss on ignition	0.82		
		insoluble/HCl	0.33		
		free CaO	0.65		

Results of the X-ray diffraction phase analysis are given in Figures 1 to 3. (Characteristic sections of diffractograms are shown in the figures). The obtained diffractograms show changes in the profiles of the recorded diffractive lines, their relative intensity, and number. Thus, slag diffractograms (Figure 1) indicate a change in the profile of diffraction lines, which correspond to the (Mn,Mg)<sub>2</sub>SiO<sub>4</sub> phase. As for the clinker sample (Figure 2), the most distinct changes were observed in the profiles of diffraction lines corresponding to the 3CaO·SiO<sub>2</sub> phase, and in the plaster sample (Figure 3) to the CaSO<sub>4</sub>·2H<sub>2</sub>O phase. The changes were less detectable in the profiles of diffraction lines corresponding to other identified phases.

The recorded changes resulting from exposure to radiation are implied by the change in FWHM value of the characteristic diffraction line profile of the reflection 004 of (Mn,Mg<sub>2</sub>)SiO<sub>4</sub> (slag), 312 of 3CaO·SiO<sub>2</sub> (clinker) and

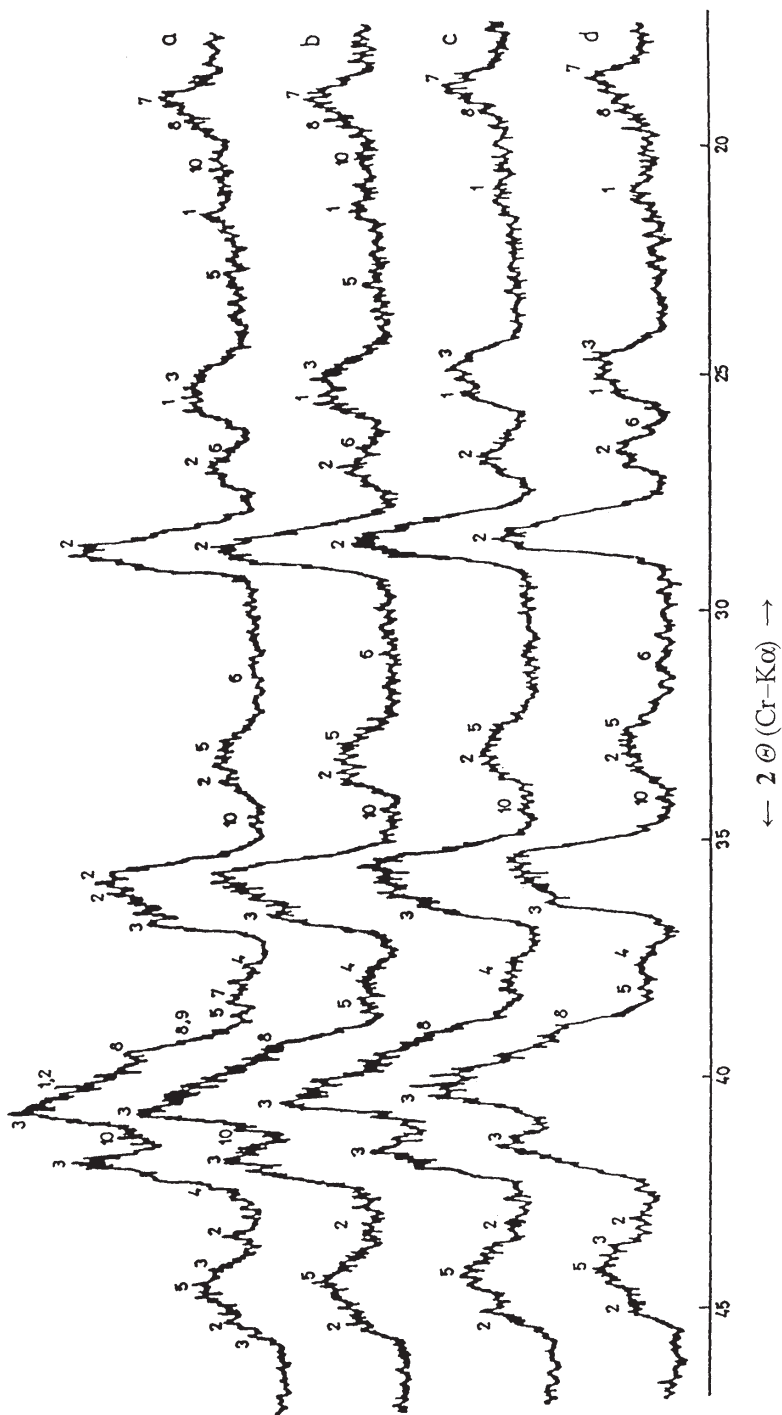


Figure 1. X-ray diffraction patterns of the slag sample before irradiation (a) and after irradiation with the primary X-ray beam for 1 hour (b), 3 hours (c), and 5 hours (d).  
 Identified phases: 1: MnO; 2: MnO · SiO<sub>2</sub>; 3: (Mn, Mg)<sub>2</sub>SiO<sub>4</sub>; 4: Mn<sub>3</sub>O<sub>4</sub>; 5: 3CaO · 2SiO<sub>2</sub>; 6: MgSiO<sub>3</sub>; 7: αCaO · SiO<sub>2</sub>; 8: CaO · Fe<sub>2</sub>O<sub>3</sub>; 9: 2FeO · SiO<sub>2</sub>; 10: MnFe<sub>2</sub>O<sub>4</sub>.

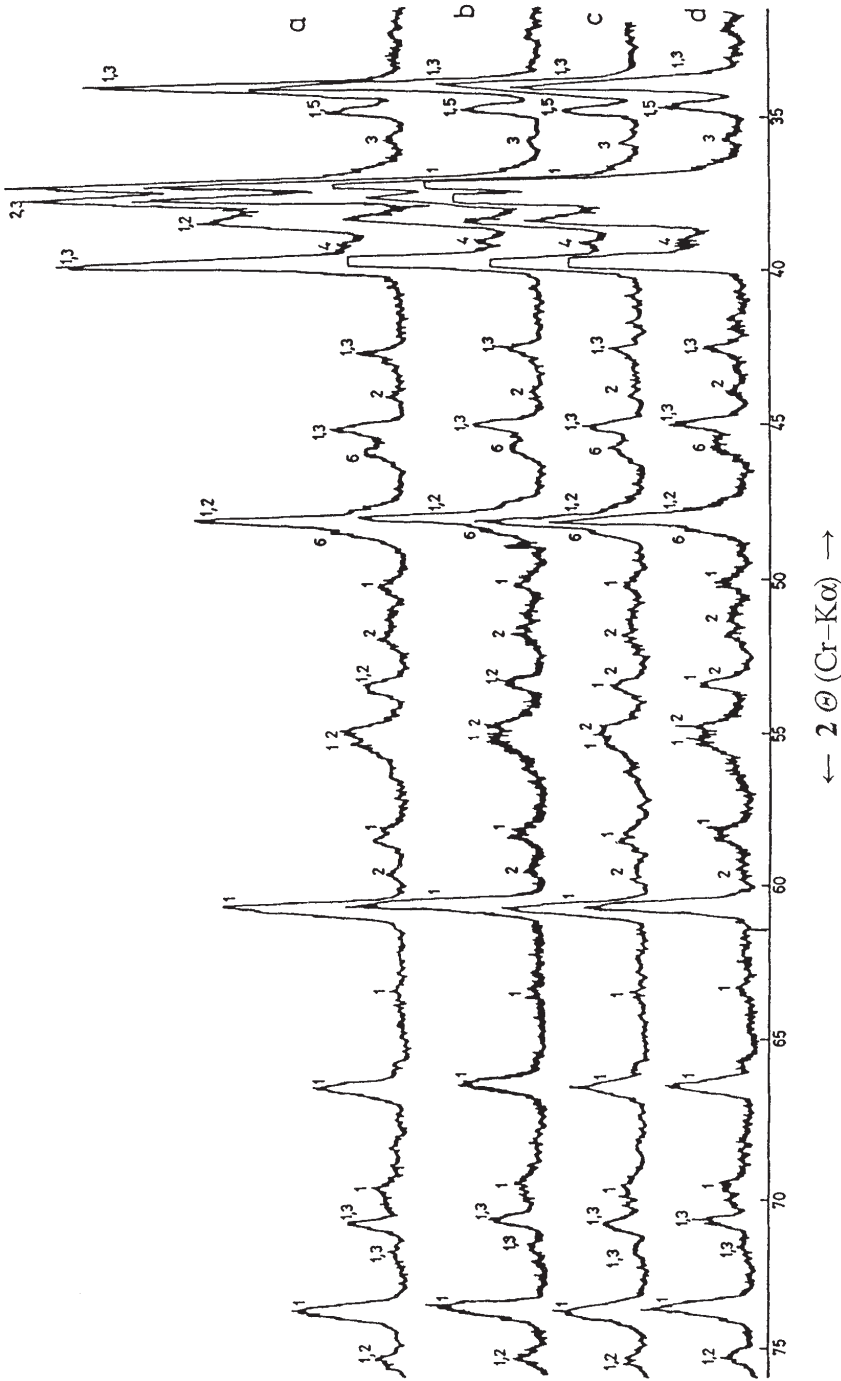


Figure 2. X-ray diffraction patterns of the clinker sample before irradiation (a) and after irradiation with the primary X-ray beam for 1 hour (b), 3 hours (c), and 5 hours (d).  
 Identified phases: 1:  $3\text{CaO}\cdot\text{SiO}_2$ ; 2:  $\alpha\text{2CaO}\cdot\text{SiO}_2$ ; 3:  $\gamma\text{2CaO}\cdot\text{SiO}_2$ ; 4:  $\alpha\text{Fe}_2\text{O}_3$ ; 5:  $2\text{CaSO}_4\cdot\text{H}_2\text{O}$ ; 6:  $\text{Ca}_3\text{Al}_2(\text{OH})_2$ .

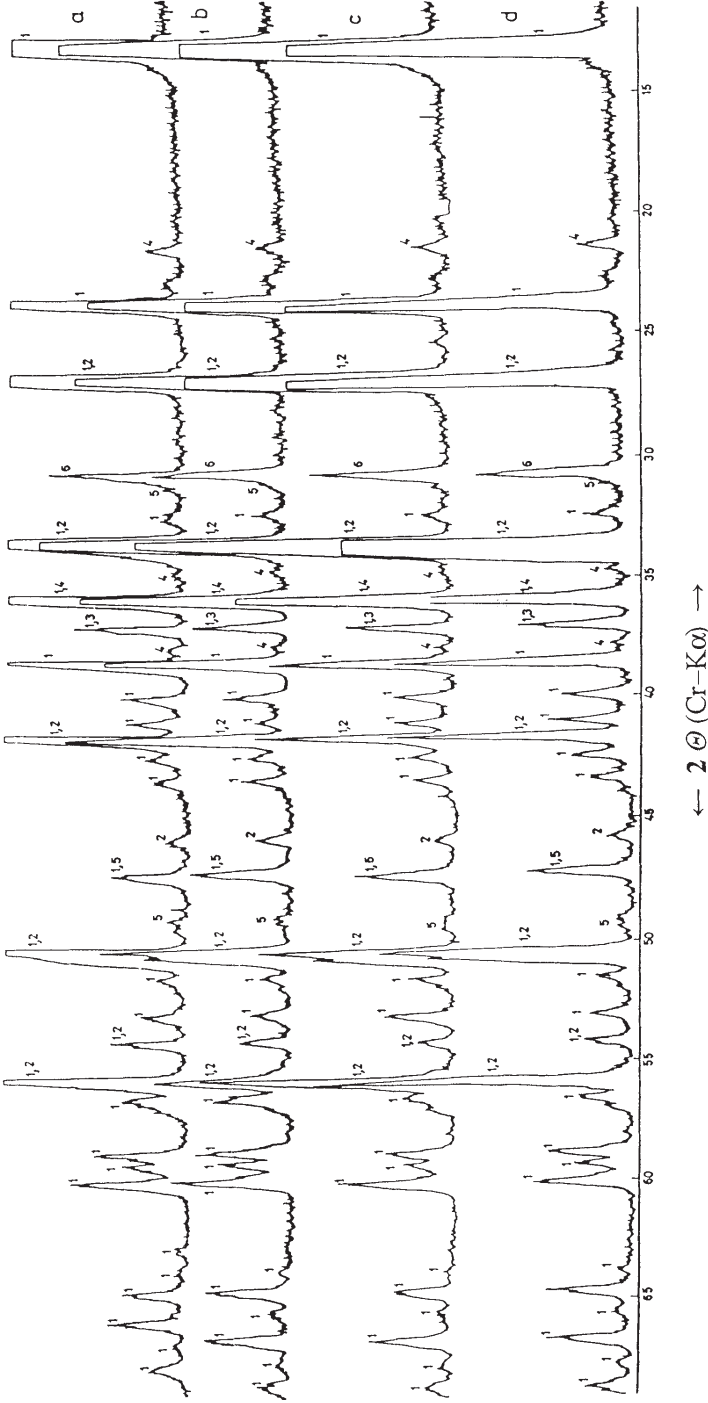


Figure 3. X-ray diffraction patterns of the plaster sample before irradiation (a) and after irradiation with the primary X-ray beam for 1 hour (b), 3 hours (c), and 5 hours (d).  
 Identified phases: 1:  $\text{CaSO}_4 \cdot 2\text{H}_2\text{O}$ ; 2:  $\text{CaCO}_3$ ; 3:  $\text{FeCO}_3$ ; 4:  $3\text{CaO} \cdot \text{Al}_2\text{O}_3 \cdot \text{CaSO}_4 \cdot 13\text{H}_2\text{O}$ ; 5:  $\text{SiO}_2$ ; 6:  $3\text{Al}_2\text{O}_3 \cdot 2\text{SiO}_2$ .

TABLE II  
FWHM values for different time of radiation in slag, clinker and plaster

Sample	Time of radiation / hours			
	0	1	3	5
	FWHM / °2θ			
slag	1.090	1.150	1.220	1.140
clinker	0.308	0.335	0.347	0.349
plaster	0.342	0.330	0.243	0.254

123 of  $\text{CaSO}_4 \cdot 2\text{H}_2\text{O}$  (plaster), as well. This is shown in Table II. The FWHM value within individual samples does not change uniformly. Thus, in the slag sample, the FWHM value of the 004 reflection of  $(\text{Mn,Mg})_2\text{SiO}_4$  increases from  $1.09^\circ 2\theta$  (not exposed sample) to  $1.22^\circ 2\theta$  (after three-hour exposure) and then it decreases to  $1.14^\circ 2\theta$  (after five-hour exposure). In the clinker sample, the FWHM value of the 312 reflection of  $3\text{CaO} \cdot \text{SiO}_2$  gradually grows from  $0.308^\circ 2\theta$  to  $0.349^\circ 2\theta$  as the exposure time increases. The plaster sample's FWHM of the 123 reflection of  $\text{CaSO}_4 \cdot 2\text{H}_2\text{O}$  decreases from  $0.342^\circ 2\theta$  (not exposed sample) to  $0.243^\circ 2\theta$  (after three-hour exposure) and then grows to  $0.254^\circ 2\theta$  (after five-hour exposure).

According to Warren and Averbach, the observed changes in FWHM values result from the microstructural changes (crystallite fragmentation and/or microstresses produced in the crystal lattice) induced exclusively by exposure to radiation.<sup>13</sup> According to Tucker and Sieno, although the recorded diffractograms indicate still good crystallinity, some changes occurred, nevertheless, as a consequence of exposure to radiation.<sup>14</sup> The research results influence of radiation on samples of cellulose, starch, and graphite point to changes in grain size and shape.<sup>15-17</sup> Analogous phenomena were detected by scanning electron microscopy on the samples of slag, clinker, and plaster exposed to radiation (Figures 4 to 6). The obtained micrographs show a morphological change of small grains, cracks, and adhesive substances. When applying slag, clinker, and plaster in construction industry, one has to consider the observed changes in the properties of such materials due to radiation.

## CONCLUSION

The influence of radiation time on samples of slag, clinker, and plaster as cement ingredients was examined. Diffractograms of the exposed sam-



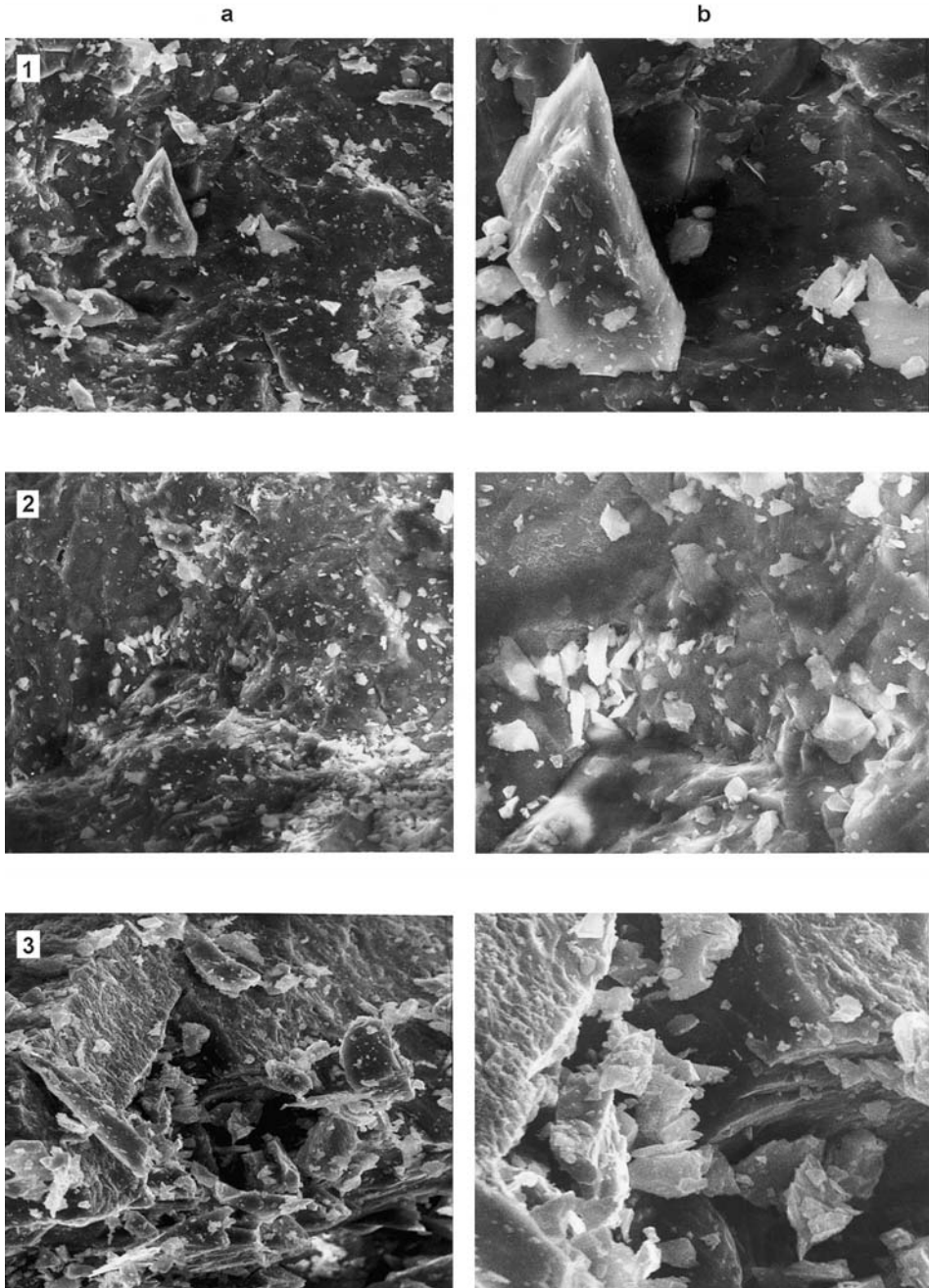


Figure 4. Scanning electron micrographs of the slag sample: (1) after irradiation for 1 hour; (2) after irradiation for 3 hours; (3) after irradiation for 5 hours; Magnification: (a) 500 x; (b) 1500 x.

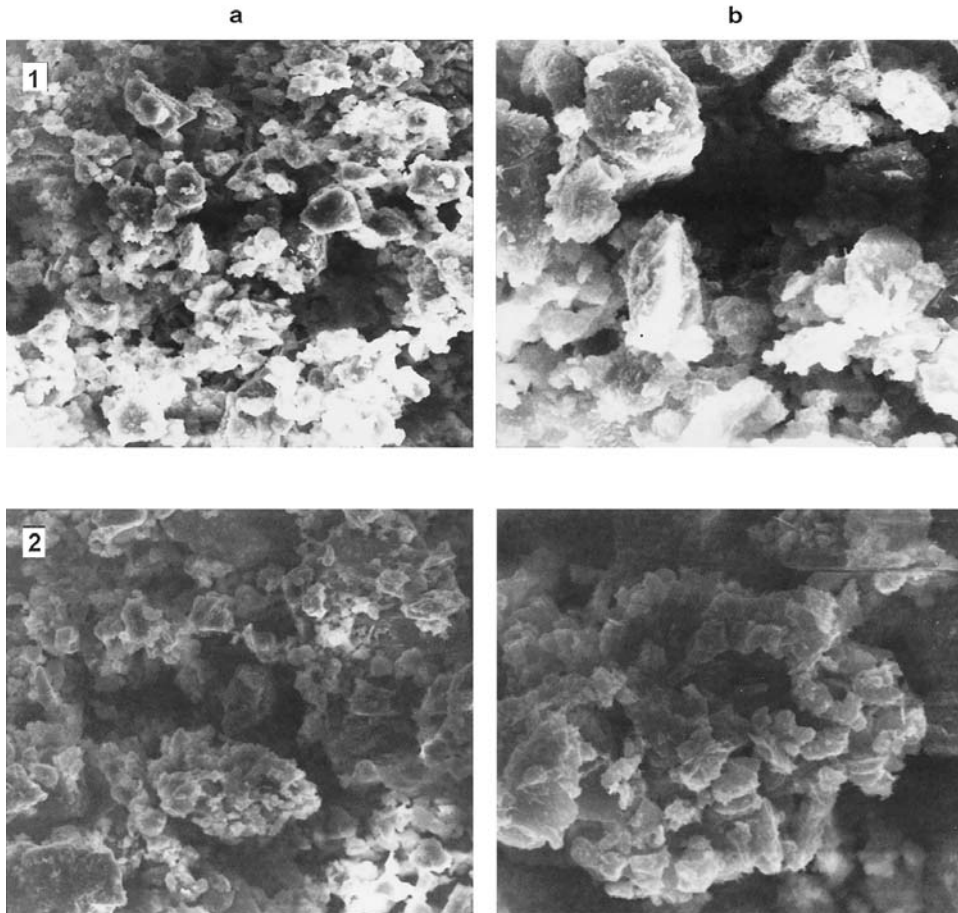


Figure 5. Scanning electron micrographs of the clinker sample: (1) after irradiation for 1 hour; (2) after irradiation for 5 hours; Magnification: (a) 500 x; (b) 1500 x.

ples, compared to the non-exposed samples, show a change in the number and intensity of recorded diffraction lines and in their FWHM. Changes caused by radiation are recorded on the scanning electron micrographs in the form of grain swelling and cracking, as well as emergence of grains in various forms and sizes. Based on the available references and obtained results, it can be concluded that the alterations recorded on the examined samples resulted from radiation-induced micro-structural changes. According to the latest references, these alterations directly affect the mechanical properties of material and accelerate the ageing process.

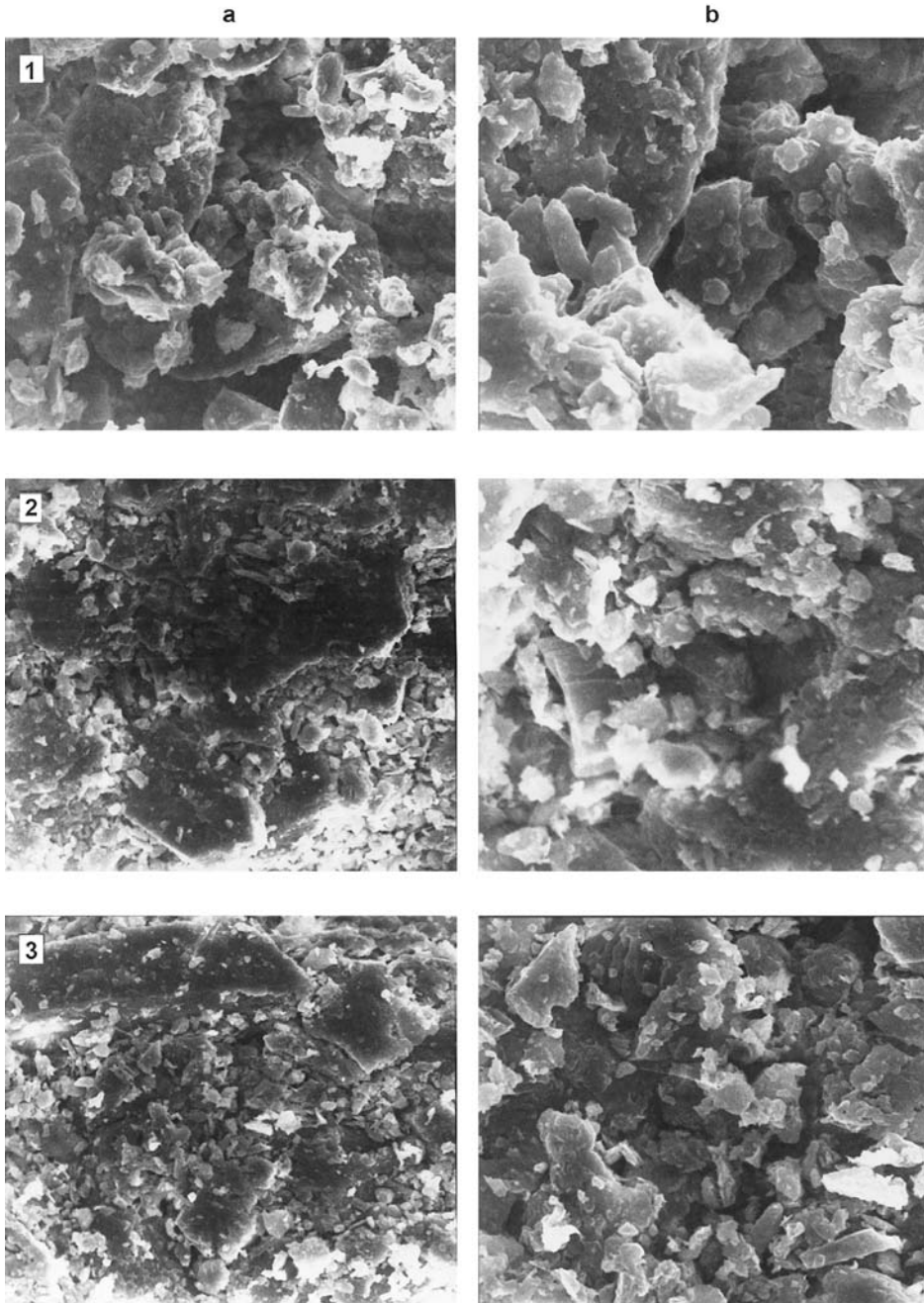


Figure 6. Scanning electron micrographs of the plaster sample: (1) after irradiation for 1 hour; (2) after irradiation for 3 hours; (3) after irradiation for 5 hours; Magnification: (a) 500 x; (b) 1500 x.



## REFERENCES

1. D. W. Lewis, *History of Slag Cements*, Slag Cement Seminar, University of Alabama, Alabama, 1981, pp. 181–186.
2. F. M. Lea, *The Chemistry of Cement and Concrete*, Edward Arnold Publishers, London, 1976.
3. J. Geiseler and S. R. Schlosser, *Investigation Concerning Structure and Properties of Steel Slags*, 3rd International Conference on Molten Slags and Fluxes, Glasgow, 1988, pp. 66–69.
4. Š. Cerjan-Stefanović, A. Rastovčan-Mioč, and Vj. Novosel-Radović, *Metalurgija* **36** (1997) 93–99.
5. B. A. Gurovich, E. A. Kuleshova, and Y. A. Nikolaev, *J. Nucl. Mater.* **246** (1997) 91–120.
6. A. R. Kuznetsov, *Fiz. Met. Metaloved.* **85** (1998) 418–420.
7. Y. Dai, F. Carsughi, H. Ulhmarer, S. Maloy, and W. Sommer, *J. Nucl. Mater.* **265** (1999) 203–227.
8. EN 196 TEIL 2 (UDC: 666.94:691.54:620.1).
9. DIN 1164 TEIL 3 (UDC: 666.96:691.55:620.1).
10. H. P. Klug and L. E. Alexander, *X-ray Diffraction Procedures for Polycrystalline and Amorphous Materials*, John Wiley and Sons, New York, 1974, pp. 365–376.
11. International Centre for Diffraction Data, Newtown Square, PA 19073–3273, USA, Powder Diffraction File.
12. K. Narita, *Kristaličeskaja Struktura Nemetaličeskikh Vključenij v Stali*, Metalurgija, Moskva, 1966, p. 59, 61, 63.
13. B. E. Warren and B. L. Averbach, *J. App. Phys.* **23** (1952) 496–501.
14. C. W. Tucker and P. Sieno, *Acta Cryst.* **7** (1954) 456.
15. Vj. Novosel-Radović, Da. Maljković, and N. Nenadić, *Spectrochim. Acta* **40B** (1985) 701–704.
16. Vj. Novosel-Radović, Da. Maljković, and N. Nenadić, *Fresenius Z. Anal. Chem.* **320** (1985) 159–162.
17. Vj. Novosel-Radović and Da. Maljković, *Chemia* **7–8** (1998) L15.

## SAŽETAK

**Utjecaj rentgenskog zračenja na fazni sastav i morfologiju elektropećne troske, klinkera i gipsa**

*Alenka Rastovčan-Mioč, Štefica Cerjan-Stefanović, Vjera Novosel-Radović, Boro Mioč i Tahir Sofilić*

Provedena su istraživanja utjecaja rentgenskog zračenja na strukturu i morfologiju uzoraka klinkera, gipsa i elektropećne troske dobivene u procesu proizvodnje austenitnog manganskog čeličnog lijeva, kako bi se odredila stabilnost tih materijala prema zračenju.

Nastale promjene analizirane su uporabom rentgenske difrakcije i elektronske mikroskopije. Na difrakcijskim slikama zapažene su promjene profila, broja i relativnog intenziteta difrakcijskih linija te izmjerene širine na polovici visine maksimuma. Na dobivenim mikrografijama uočava se pojava bubrenja i pucanja zrna. S porastom vremena ozračivanja ta pojava biva sve više izražena i dovodi do izrazite promjene veličine i oblika zrna osnovnih komponenata cementa, tj. troske, klinkera i gipsa.